P- ISSN 1991-8941 E-ISSN 2706-6703
2024,(18), (02):203 – 212

Journal of University of Anbar for Pure Science (JUAPS) Open Access

Characterization of Nickel Oxide Nanoparticles Prepared Via Pulsed Laser Ablation: Evaluation of the Influence of Laser Parameters

Bushra Mohammed Ghdhaib , Sahar Naji Rashid *

Department of Physics, College of Science, Tikrit University, Tikrit, Iraq;

ARTICLE INFO

Received: 30 / 03 /2024
Accepted: 30/ 06 /2024
Available online: 26/ 12 /2024

10.37652/juaps.2024.148124.1224

Keywords:
Laser parameters; NiO NPs; PLAL; SPR

ABSTRACT

Top-down pulsed laser ablation in liquids has many advantages in the synthesis of nanoparticles (NPs). In this work, NPs of pure nickel (Ni) plate were prepared via pulsed laser ablation in deionized water, with the utilization of Nd:YAG laser with three wavelengths (1064, 532, and 355 nm) and three energies (50, 100, and 150 mJ). The results demonstrate the formation of Ni NPs in addition to spherical nickel oxide NPs with average sizes of 14.3–18.44 nm. The oxidation rate increased when the shorter wavelength of the laser was used in the preparation. The intensity of absorption rose with the increase in laser energy. The best wavelength used for the preparation was 532 nm, and the best energy was 150 mJ. This physical technique has proven its advantage in terms of ease and low-cost preparation of metal NPs and their nano oxides and regulation of their properties by controlling the laser and ablation parameters.

Introduction

Pulsed laser ablation in liquids (PLAL) has become widely used in the preparation of nanoparticles (NPs) because it is an easy, fast, and low-cost approach; in addition, it enables the control of the properties, morphology, shape, and size of NPs in one step [1-7]. PLAL technique employs several parameters (including laser parameters), which are responsible for controlling the properties of the resulting NPs, such as wavelength, energy, the number of pulses, types, and quantity of liquid medium [8-12]. The properties of the material are generally affected by the thermal stress that results from the mechanism of spread and temperature distribution during its absorption of laser beams [13]. PLAL technology enables the interaction of the laser beam with the surface of the material present in the liquid medium and creates conditions conducive to the production of a plasma column immersed in the medium. This condition leads to the production of unique thermodynamic conditions with high temperature and pressure that allow NP production [11,14].

When the metal target is exposed to a high laser fuel, the free electrons oscillate collectively on the target surface, which causes absorption and scattering depending on the wavelength. Metal NPs can absorb light in the visible range by creating a collective vibration of conduction bands, which is in strong resonance with specified frequencies of light. This unique feature of metallic NPs is called surface plasmon resonance (SPR), where the electromagnetic field in the surroundings is enhanced by plasmon excitation and produces measurable changes in NPs in the optical field [5,14]. Metal NPs possess unusual electrical and optical properties and catalytic activity, in addition to their high bactericidal effect. These remarkable properties are determined by the size, shape, and spatial organization of nano-objects and depend on formation conditions [15]. Nickel (Ni) NPs have been the topic of vast research on numerous applications because of their properties, such as extreme catalytic activity, high compressive strength, superior ferromagnetic properties, and antibacterial effects [16-21]. In addition, nickel oxide NPs (NiO NPs) have acquired massive attention in various scientific fields for their physical, chemical, and biological properties [22-27]. This work aimed to evaluate the effect of changes in some laser parameters, specifically energy and

*Corresponding author at : Department of Physics, College of Science, Tikrit University, Tikrit, Iraq
ORCID:https:// **https://orcid.org/0000-0001-7559-3435** ,
Tel: +9647709507060
Email: sahar83@tu.edu.iq

wavelength, on the optical and structural properties of NPs prepared from a pure Ni plate using the Nd:YAG pulsed laser ablation technique to determine the appropriate energy and wavelength under current working conditions and obtain NPs with low size rates and high absorption.

Materials and Methods

Nd:YAG laser with wavelengths of 1064, 532, and 355 nm and energies of 50, 100, and 150 mJ for each wavelength, repetition rate (3 Hz), and 500 pulses was used to prepare three solutions containing colloidal NPs in 3 ml deionized water. A pure Ni metal plate with dimensions of 1 cm × 1 cm × 1 mm was utilized, and the liquid (1 cm) and source (15 cm) levels were above the target.

To determine the extent of wavelengths and energy influences on the most important structural and optical characteristics of the prepared NP colloidal solution, we detected the properties using several important techniques; X-ray diffraction (XRD) was used to determine the crystalline structure, and the average crystal size of the prepared NPs was obtained using the Debye–Scherrer equation [4]:

$$D = 0.9\lambda/\beta\cos\theta \qquad (1)$$

where λ denotes the wavelength of the X-ray (1.54060 Å), θ indicates the angle of diffraction, and β is the full width at half maximum of the diffraction peaks under various laser fluencies. To obtain the NP shape, we determined the diameters of the prepared NPs, active groups, colloidal solution compositions, absorbance (A), and transmittance (T) spectra and calculated the component proportions of the colloidal solutions. Some of the most important techniques were used: field emission scanning electron microscope (FESEM), Fourier transform infrared spectroscopy, ultraviolet-visible spectrophotometer, and dispersive X-ray spectroscopy. By taking advantage of the optical spectra resulting from spectrophotometry and depending on the length of beam path inside the glass cuvette containing the nanocolloidal solution, some optical constants, such as the optical conductivity (σ), were calculated using Equation (2), and the energy gap was computed using Tauc equation (3) [28].

$$\sigma = \alpha nc/4\pi \qquad (2)$$

$$\alpha h\upsilon = B(h\upsilon - E_g)^{\frac{1}{2}} \qquad (3)$$

where α represents the absorption coefficient, c denotes the light velocity, n indicates the refractive index, B is a constant, h stands for the Planck constant, Eg means the energy gap, and υ is the photon frequency.

Results and Discussion

The outcomes of XRD of nanocolloidal solutions prepared via laser ablation at three wavelengths at the energy of 150 mJ for each wavelength showed the formation of Ni NPs with a cubic phase (JCPDS Card No. 00-001-1260), in addition to NiO NPs with two dominant phases, namely, cubic NiO NPs (JCPDS Card No. 47-1049) and hexagonal nickel trioxide NPs (Ni_2O_3 NPs; JCPDS Card No. 00-014-0481) (Figure 1). The formation of metal oxide NPs was attributed to the reactions between the ejected Ni and the surrounding liquid [1], [9], where the NPs of oxides resulted from the metal atoms' interaction with radicals or oxygen atoms during dissolution in the liquid depending on the partial pressure of oxygen and temperature [29]; this condition also explains the appearance of additional peaks given that X-rays were scattered by the electrons of air atoms surrounding the liquid medium itself. The figure shows that the nanonickel oxide phases dominated compared with nanonickel. This finding implies the large surface oxidation rate of the NPs formed. Regardless, the survival of nanonickel indicates the possible completion of the chemical reactions between the extruded Ni and the surrounding liquid during NP formation. Table 1 shows that the average crystal sizes of the prepared NPs calculated using Equation (1) were 14.6, 12, and 15 nm at the wavelengths of 1064, 532, and 355 nm, respectively, which means that preparation at the wavelength of 532 nm produced NPs with a smaller average size. Meanwhile, the use a lower wavelength (532 nm) resulted in an increase in the laser flux, which caused a reduction in the average crystal sizes of the resulting NPs [9]; however, the continued increase in laser flux (which was obtained using a lower wavelength 355 nm) led to an increase in the ablation rate. Thus, NP aggregation occurred, and it led to an increased rate of their size.

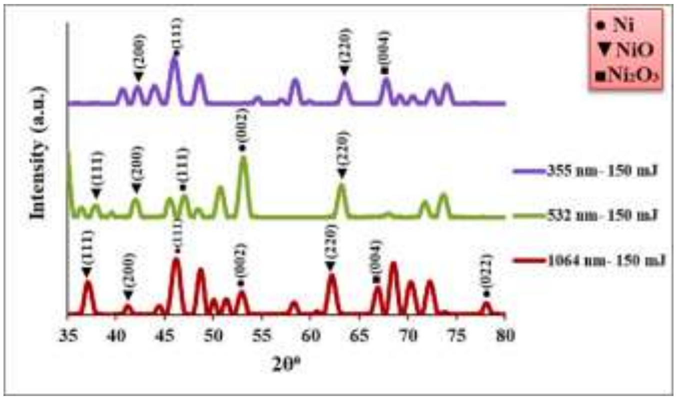

Figure 1. XRD pattern of the prepared NPs

Table 1. XRD analysis results of prepared NPs

λ (nm)	NPs	2θ (deg)	hkl	β (deg)	d (nm)	D (nm)
1064	NiO	37.15	111	0.6	0.241724	13.96268
1064	NiO	41.2	200	0.5	0.218848	16.96729
1064	Ni	46.2	111	0.8	0.19626	10.79176
1064	Ni	52.95	002	0.7	0.17272	12.67366
1064	NiO	62.2	220	0.8	0.149071	11.59275
1064	Ni_2O_3	66.95	004	0.6	0.139601	15.86729
1064	Ni	78	022	0.5	0.122354	20.43682
532	NiO	37.9	111	0.6	0.237111	13.99375
532	NiO	42	200	0.7	0.214863	12.15167
532	Ni	47	111	0.6	0.193104	14.43234
532	Ni	53	002	0.8	0.172569	11.09187
532	NiO	63.2	220	0.8	0.146951	11.65455
355	NiO	42.2	200	0.6	0.213891	14.18648
355	Ni	46	111	0.6	0.197066	14.37833
355	NiO	63.5	220	0.6	0.146328	15.56452
355	Ni_2O_3	67.7	004	0.6	0.138235	15.9366

the results of FESEM of nanocolloidal solutions prepared via laser ablation at the energy of 150 mJ and wavelengths of 1064, 532, and 355 nm, respectively. The figures reveal the surface morphology of the samples prepared at the scale of 100 nm and the spherical shape of the resulting NPs, which is in agreement with the finding of other studies [8], [9]; the average diameters reached 16.53, 14.78, and 21.73 nm for the NPs prepared at wavelengths of 1064, 532, and 355 nm, respectively. In addition, the figures show the distribution sizes, with the average sizes reaching 15.18, 14.3, and 18.44 nm during NP preparation at wavelengths of 1064, 532, and 355 nm, respectively, which is consistent with the results of XRD analysis, where lower average diameters were observed when NPs were prepared at the wavelength of 532 nm. Aggregation formation can also be observed, that is, clusters composed of two or more NPs were observed. NPs induced aggregation; large particles can be formed through their combination, and they settled via gravitational force, which enabled their collision and formation of larger clusters.

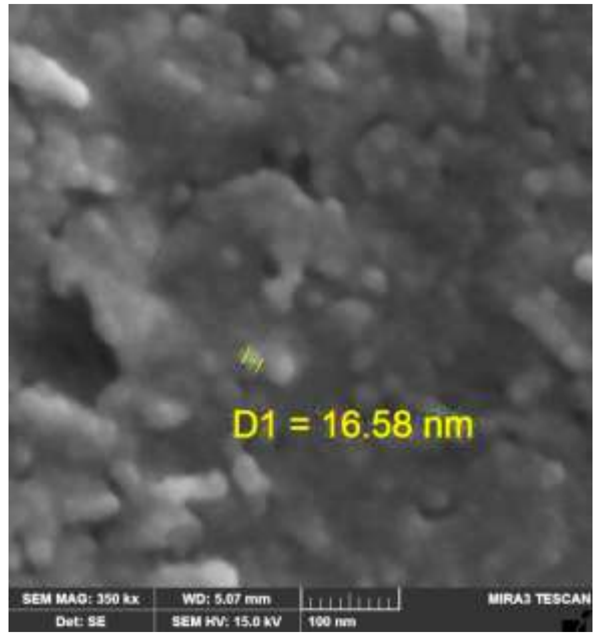

(a)

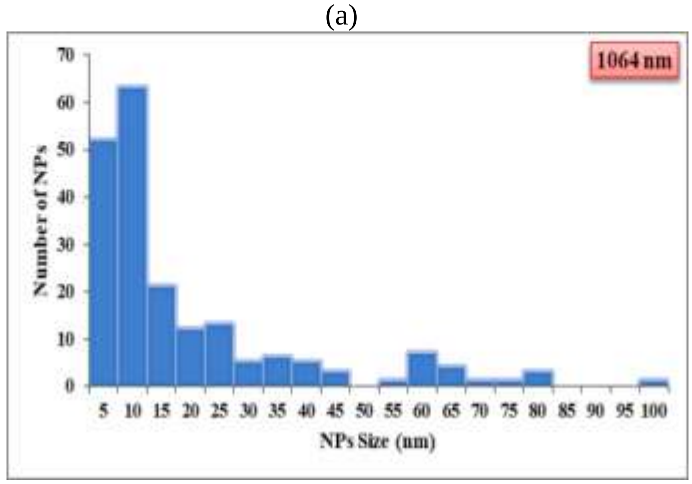

(b)

Figure 2. FESEM image of prepared NPs at 1064 nm: a) at the scale 100 nm, b) size distribution

(a)

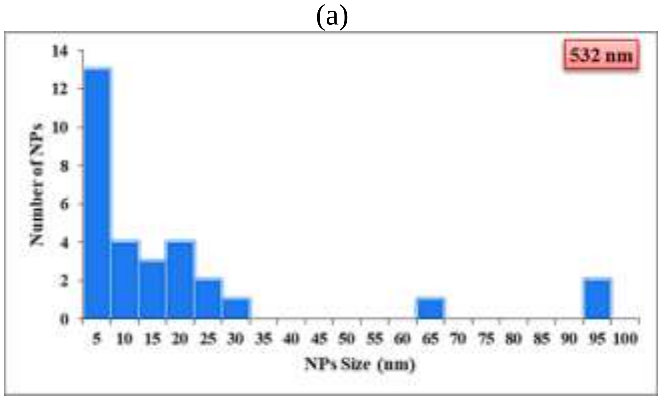

(b)

Figure 3. FESEM image of prepared NPs at 532 nm: a) at the scale 100 nm, b) size distribution

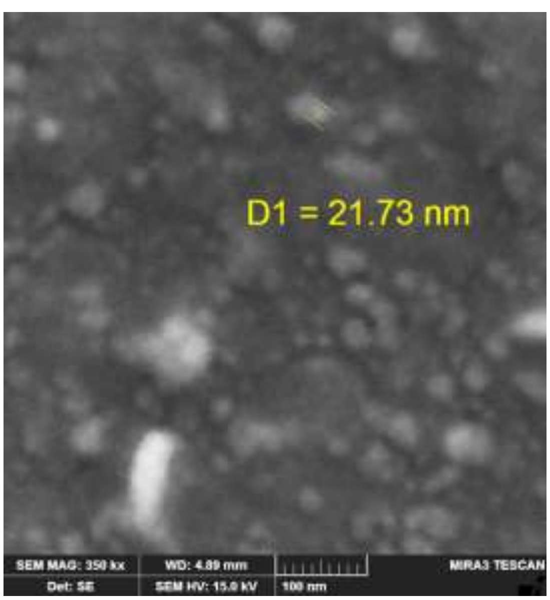

(a)

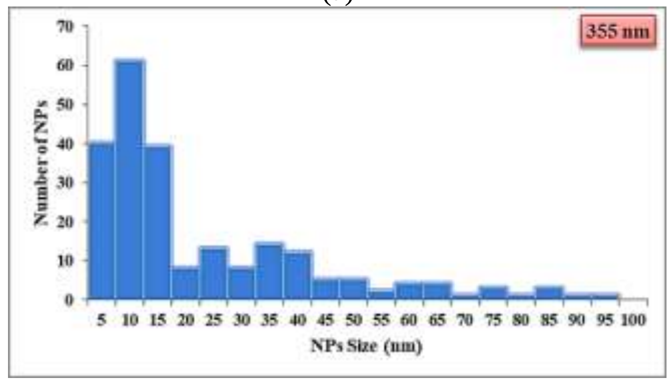

Figure 4. FESEM image of prepared NPs at 355 nm: a) at the scale 100 nm, b) size distribution

Analysis of the elemental composition of the prepared samples at 150 mJ revealed an increase in oxidation rates, consistent with the results of XRD analysis (Figures 5, 6, and 7), where the weight and atomic percentages and k-ratio of oxygen increase observed with the increase in the laser wavelength used in sample preparation were calculated based on the weight and atomic percentages and k-ratio of Ni (Table 2).

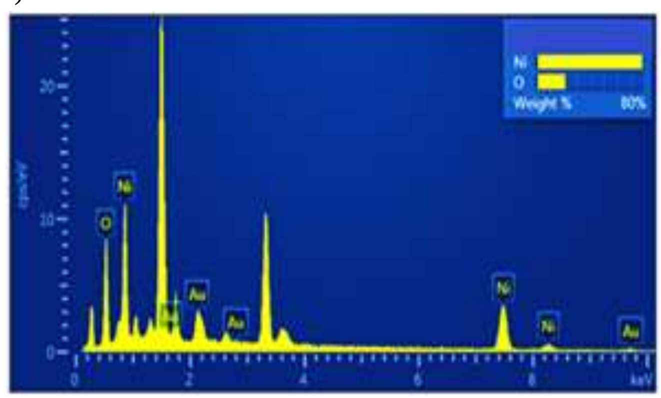

Figure 5. EDX analysis of prepared NPs at 1064 nm

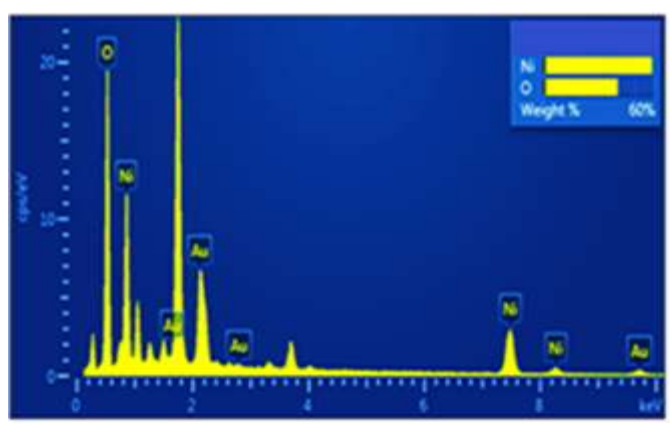

Figure 6. EDX analysis of prepared NPs at 532 nm

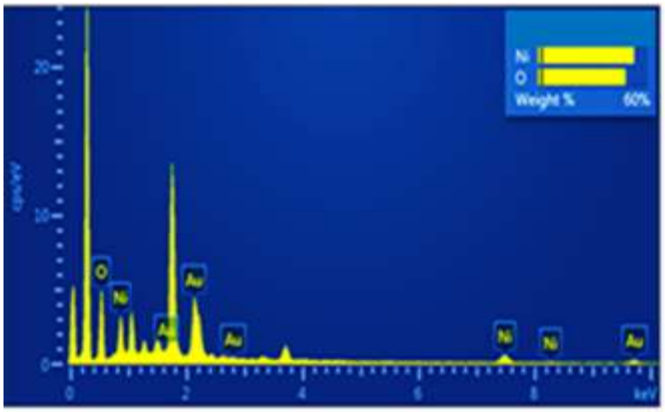

Figure 7. EDX analysis of prepared NPs at 355 nm

Table 2. EDX analysis results of prepared NPs

λ (nm)	Element	k-ratio	Weight (%)	Atomic (%)
1064	O	0.00765	21.47	50.08
1064	Ni	0.05537	78.53	49.92
532	O	0.01836	40.54	71.44
532	Ni	0.04645	59.46	28.56
355	O	0.00447	47.64	76.95
355	Ni	0.00804	52.36	23.05

Figures 8, 9, and 10 present the curves of some properties and optical constants of NPs prepared at wavelengths of 1064, 532, and 355 nm respectively. In addition to the widening of the peak width, the intensity of the absorption spectrum increased with the increase in the preparation energy, which is in agreement with the findings of other studies [6,30]. These peaks, which represent SPR, corresponded to that detected at the wavelength of 300 nm. These peaks appeared due to a frequency matching the incident-light photons and surface electrons of the NPs, which accounted for the emergence of a brown color; the tendency for dark brown color was also observed with the increase in laser energy as a result of the increased concentration of NPs in the colloids [1]. As a result of the behavior of the absorption spectrum, the transmittance spectrum behaved oppositely. As for the optical conductivity of the prepared NPs, the peaks were approximately observed in the SPR region, and their value was affected by ablation parameters as it increased with the increase in preparation energy. The optical properties of the prepared samples were related to their structural properties. Thus, changing the composition of the samples affected their optical properties. Given that the appearance of metal oxide NPs detected in the XRD analysis of the prepared samples implies the formation of an energy gap, the values generally increased with the increase in the preparation energy except for those prepared at the wavelength of 355 nm. In general, the behavior of the optical properties curves of the prepared NPs applies to the samples prepared at all wavelengths.

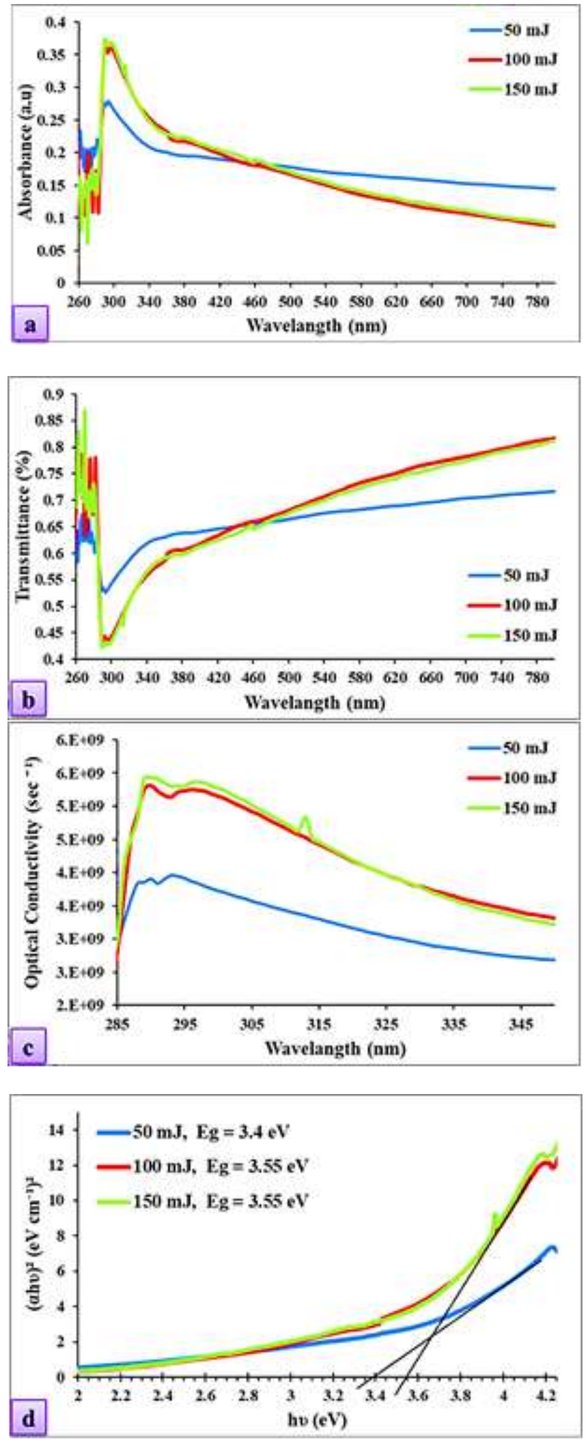

Figure 8. UV-Vis spectrophotometer analysis of prepared NPs at 1064 nm: a) Absorbance, b) Transmittance, c) Optical conductivity, d) Energy gap

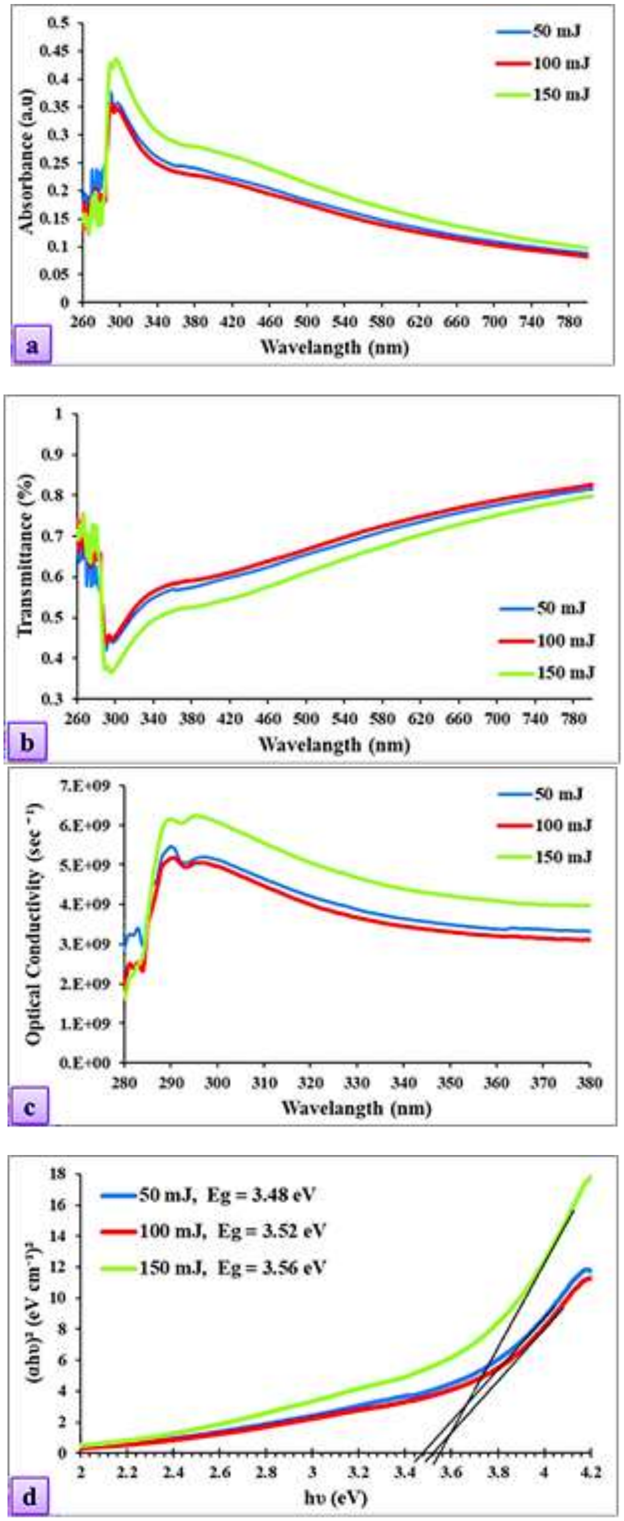

Figure 9. UV-Vis spectrophotometer analysis of prepared NPs at 532 nm: a) Absorbance, b) Transmittance, c) Optical conductivity, d) Energy gap

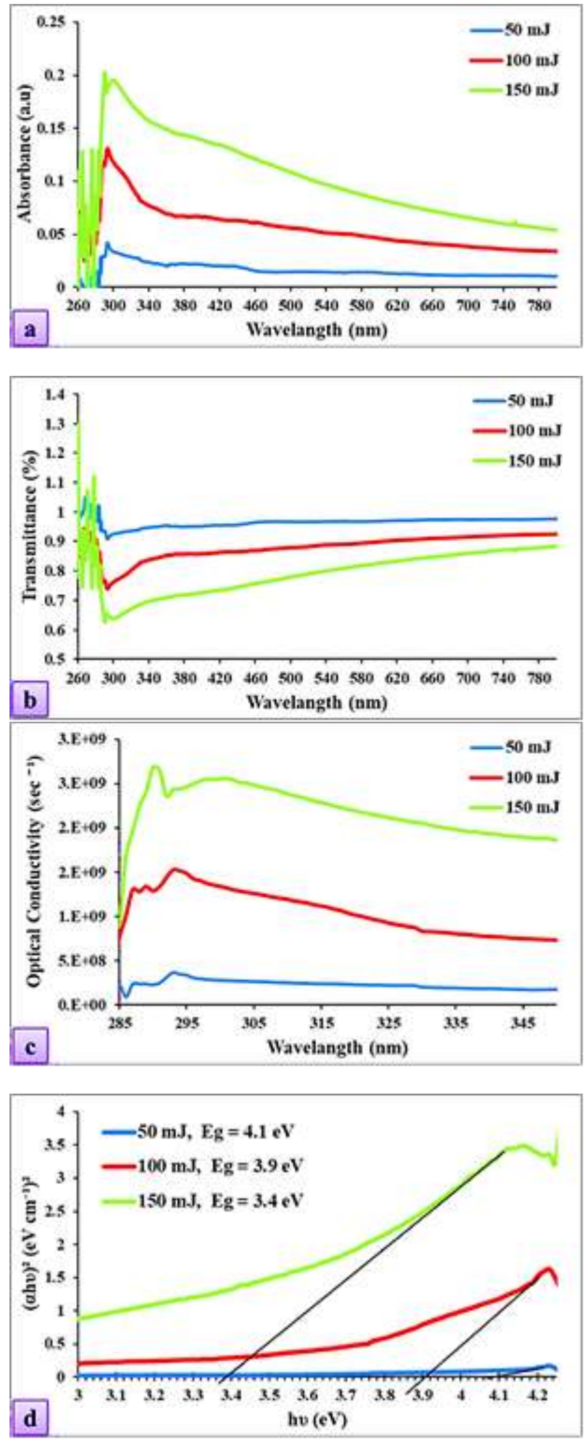

Figure 10. UV-Vis spectrophotometer analysis of prepared NPs at 355 nm: a) Absorbance, b) Transmittance, c) Optical conductivity, d) Energy gap

The structural properties demonstrated that the obtained nanocolloidal solutions comprised Ni NPs, NiO NPs, and Ni_2O_3 NPs. Thus, the absorption peaks of these colloidal solutions, which represent SPR, belonged to the Ni NPs. The calculated energy gaps were the direct energy gap, which was due to the NiO NPs that dominated the prepared samples, as shown by the results of XRD analysis. The energy gap increased with the decrease in NP sizes due to nanoscale electron confinement, that is, the quantum size effect, which means that electrons were confined and occupied less space than bulk. The results show that the energy gaps (3.48–3.56 eV) calculated at the wavelength of 532 nm in the preparation process were higher than those calculated at the wavelength of 1064 nm (3.4–3.55 eV). This finding is consistent with that of of FESEM analysis, which revealed that the average NP sizes were smaller when the wavelength of 532 nm was used in the preparation. Meanwhile, the use of the 355 nm wavelength in the preparation led to an increase in the energy gap (compared with the other two wavelengths), with values in the range of 3.4–4.1 eV. This finding was due to an increase in the average size of the prepared NPs caused by the aggregation and agglomeration resulting from the increase in laser flow.

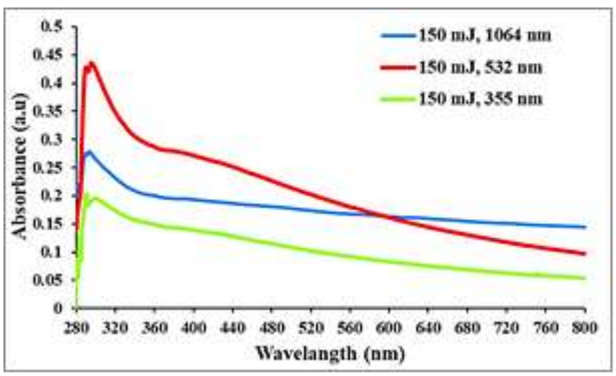

Figure 11. Comparison of the absorption spectrum of prepared NPs at the highest preparation energy

Finally, during the comparison of the absorption spectra of the prepared NPs at the highest preparation energies at the three wavelengths (Figure 11), the highest peak was observed for the NPs prepared at the wavelength of 532 nm, which indicates that this wavelength is the best for the preparation of Ni NPs and NiO NPs within the current working environment; this condition led to smaller average sizes, with the higher peak and its widening indicating the smaller size of the NPs, similar to previous studies [31,32]; such finding was observed in the results of XRD and FESEM analyses.

Conclusions

The capability of pulsed laser ablation technique for the preparation of NPs has been proven, with the possibility of regulating their physical properties through the control of laser and ablation parameters. The results of structural and optical measurements of Ni NPs and NiO NPs reveal that the use of a short wavelength and high energy of the laser led to increases in the oxidation rate and concentration of the NPs, which resulted in their aggregation. The energy gap of NiO NPs increased with the decrease in NP sizes due to nanoscale electron confinement, that is, the quantum size effect. The current conditions of this work revealed that 532 nm and 150 mJ are the most suitable wavelength and laser energy for NP preparation, respectively. Although the first and third harmonics of the laser provided desirable results, the second harmonic was the best, the findings of which can be used in biological and industrial applications.

Acknowledgments

The authors extend their sincere thanks and gratitude to the Department of Physics at the College of Science at Tikrit University for providing the opportunity and the required equipment in its optics and laser laboratory to conduct this work

Conflict of Interest

Authors declare that they have no conflict interests.

References

[1] Khashan, K. S., Sulaiman, G. M., Hamad, A. H., Abdulameer, F. A. & Hadi, A. (2017). Generation of NiO nanoparticles via pulsed laser ablation in deionised water and their antibacterial activity. *Applied Physics A*, *123*(190), 1-10. https://doi.org/10.1007/s00339-017-0826-4.

[2] Iacono, V., Scuderi, M., Amoruso, M. L., Gulino, A., Ruffino, F. & Mirabella, S. (2023). Pulsed laser ablation production of Ni/NiO nanoelectrocatalysts for oxygen evolution reaction. *APL Energy, AIP Publishing*, *1*(016104), 1-8. https://doi.org/10.1063/5.0144600.

[3] Altammar, K. A. (2023). A review on nanoparticles: characteristics, synthesis, applications, and challenges. *Frontiers in Microbiology*, 14(1155622), 1-20. https://doi.org/10.3389/fmicb.2023.1155622.

[4] Hussain, N. A., Abbas, L. Y. & Latif, L. A. (2021). Preparation of Nickel Oxide Microparticles by

Pulsed Laser Ablation and Application to Gas Sensors. *Engineering and Technology Journal*, *39*(6), 1011-1018. https://doi.org/10.30684/etj.v39i6.1593.

[5] Nyabadza, A., McCarthy, E., Makhesana, M., Heidarinassab, S., Plouze, A., Vazquez, M. & Brabazon, D. (2023). A review of physical, chemical and biological synthesis methods of bimetallic nanoparticles and applications in sensing, water treatment, biomedicine, catalysis and hydrogen storage. *Advances in Colloid and Interface Science*, 321(103010), 1-44. https://doi.org/10.1016/j.cis.2023.103010.

[6] Kim, J., Reddy, D. A., Ma, R. & Kim, T. K. (2014). The influence of laser wavelength and fluence on palladium nanoparticles produced by pulsed laser ablation in deionized water. *Solid State Sciences*, 37, 96-102. https://doi.org/10.1016/j.solidstatesciences.2014.09.005.

[7] Seifikar, F., Azizian, S., Eslamipanah, M. & Jaleh, B. (2022). One step synthesis of stable nanofluids of Cu, Ag, Au, Ni, Pd, and Pt in PEG using laser ablation in liquids method and study of their capability in solar-thermal conversion. *Solar Energy*, 246, 74-88. https://doi.org/10.1016/j.solener.2022.09.040.

[8] Khashan, K. S., Saimon, J. A., Hadi, A. A. & Mahdi, R. O. (2021). Influence of laser energy on the optoelectronic properties of NiO/Si heterojunction. *Journal of Physics: Conference Series*, 1795 (012026), 1–6. https://doi.org./10.1088/1742-6596/1795/1/012026.

[9] Safa, M., Dorranian, D., Masoudi, A. A. & Matin, L. F. (2019). Characterizing nickel oxide nanostructures produced by laser ablation method: effects of laser fluence. *Applied Physics A*, *125*(687), 1-9. https://doi.org/10.1007/s00339-019-2986-x.

[10] Baladi, A. & Mamoory, A. (2012). Effect of Laser Wavelength and Ablation Time on Pulsed Laser Ablation Synthesis of Al Nano-particles in Ethanol. *International Journal of Modern Physics: Conference Series*, 5, 58-65. https://doi.org/10.1142/S2010194512001845.

[11] Mostafa, A. M. & Mwafy, E. A. (2020). The effect of laser fluence for enhancing the antibacterial activity of NiO nanoparticles by pulsed laser ablation in liquid media. *Environmental Nanotechnology, Monitoring & Management*, 14(100382), 1-8. https://doi.org/10.1016/j.enmm.2020.100382.

[12] Rashid, S. N., Mahdi, E. M. & Jasim, A. S. (2021). Effect of diode laser on ants (*Camponotus consobrinus*). *Materials Today: Proceedings*, *42*(4), 1980-1985. https://doi.org/10.1016/j.matpr.2020.12.245.

[13] Goyes, C., Ferrari, M., Armellini, C., Chiasera, A., Jestin, Y., Righini, G. C., Fonthal, F. & Solarte, E. (2009). CO_2 laser annealing on er-bium-activated glass–ceramic waveguides for photonics. *Optical Materials*, *31*(9), 1310-1314. https://doi.org./10.1016/j.optmat.2008.10.005.

[14] Rashid, S. N., Aadim., Jasim, A. S. & Hamad, A. M. (2022). Synthesized Zinc Nanoparticles via Pulsed Laser Ablation: Characterization and Antibacterial Activity. *Karbala International Journal of Modern Science*, *8*(3), 462-476. https://doi.org/10.33640/2405-609X.3240.

[15] Volkova, N. N., Bogdanova, L. M., Volkov, V. T., Karabulin, A. V., Matyushenko, V.I. & Spirin, M. G. (2021). Kinetic regularities of thermal decomposition of polycarbonate films containing Pt, Au, Ag, and Ni nanoparticles. *Russian Chemical Bulletin, International Edition*, *70*(9), 1690-1698. https://doi.org/10.1007/s11172-021-3271-7.

[16] Yahaya, N. I. S., Sapian, N. I. H., Duralim, M. B., Aziz, M. S. A., Rahman, Alias, S. S. & Husein, N. A. (2023). Synthesis of nickel nanoparticles by pulsed laser ablation in different liquid media. *International Laser Technology and Optics Symposium*, *2432*(012006), 1-9. https://doi.org./10.1088/1742-6596/2432/1/012006.

[17] Shalichah, C. & Khumaeni, A. (2018). Synthesis of nickel nanoparticles by pulse laser ablation method using Nd: YAG laser. *IOP Conf. Series: Journal of Physics: Conf. Series*, *1025*(012002), 1-4. https://doi.org./10.1088/1742-6596/1025/1/012002.

[18] Jaji, N., Lee, H. L., Hussin, M. H., Akil, H. M., Zakaria, M. R. & Othman, M. B. H. (2020). Advanced nickel nanoparticles technology: From synthesis to applications. *Nanotechnology Reviews*,

9, 1456-1480. https://doi.org/10.1515/ntrev-2020-0109.

[19] Giurlani, W., Innocenti, M. & Lavacchi, A. (2018). X-ray Microanalysis of Precious Metal Thin Films: Thickness and Composition Determination. *Coatings*, *8*(84), 1-12. https://doi.org./10.3390/coatings8020084.

[20] Hassani, M. R., Yasmin, F., Noor, F. K., Rahman, M. S., Uddin, M. S. & Bhowmik, S. (2023). Synthesis and Applications of Nickel Na-noparticles (NiNPs)- Comprehensive Review. *Journal of Ultra Chemistry*, *19*(1), 9-37. http://dx.doi.org/10.22147/juc/190102.

[21] Wawrzyniak, J. Karczewski, J. Ryl, J., Grochowska, K. & Siuzdak, K. (2020). Laser-Assisted Synthesis and Oxygen Generation of Nickel Nanoparticles. *Materials*, *13*(18), 1-13. https://doi.org./10.3390/ma13184068.

[22] Berhe, M. G. & Gebreslassie, Y. T. (2023). Biomedical Applications of Biosynthesized Nickel Oxide Nanoparticles. *International Journal of Nanomedicine*, 18, 4229-4251. https://doi.org./10.2147/IJN.S410668.

[23] Aftab, M., Butt, M. Z., Ali, D., Tanveer, M. U. & Hussnain, A. (2020). Effect of Molarity on the Structure, Optical Properties, and Surface Morphology of (002)-Oriented Ni_2O_3 Thin Films Deposited via Spray Pyrolysis. *Proceedings of the Pakistan Academy of Sciences: A. Physical and Computational Sciences*, *57*(2), 51-74. https://doi.org./10.13140/RG.2.2.17991.11683.

[24] Iacono, V., Mirabella, S., & Ruffino, F. (2023). Efficient oxygen evolution reaction catalyzed by Ni/NiO nanoparticles produced by pulsed laser ablation in liquid environment. *physica status solidi (b)*, *260*(10), 2200590(1-9). https://doi.org/10.1002/pssb.202200590.

[25] Khashan, K. S., Sulaiman, G. M., Ameer, F. A. & Napolitano, G. (2016). Synthesis, characterization and antibacterial activity of colloidal NiO nanoparticles. *Pak. J. Pharm. Sci*., *29*(2), 541-546. https://pubmed.ncbi.nlm.nih.gov/27087098/.

[26] Khairnar, S. D. & Shrivastava, V. S. (2019). Facile synthesis of nickel oxide nanoparticles for the degradation of Methylene blue and Rhodamine B dye: a comparative study. *Journal of Taibah University for Science*, *13*(1), 1108-1118. https://doi.org./10.1080/16583655.2019.1686248.

[27] Hrbe, Z. A., Alzubaidy, M. H. J., & Abd, A. N. (2022). Laser ablation of nickel oxide nanoparticles in water and its antibacterial activity. *NeuroQuantology*, *20*(7), 3028-3033. https://doi.org./10.14704/nq.2022.20.7.NQ33380.

[28] Arumanayagam, T. & Murugakoothan, P. (2011). Optical Conductivity and Dielectric Response of an Organic Aminopyridine NLO Single Crystal. *Journal of Minerals & Materials Characterization & Engineering*, *10*(13), 1225-1231. https://www.scirp.org/journal/PaperInforCitation?PaperID=20964.

[29] Rashid, S. N., Jasim, A. S., Aadim, K. A. & A. Alwan, M. A. (2023). Physical Characterization and Antibacterial Activity Evaluation of Nanoparticles Manufactured from Zinc Plate by Pulsed Laser Ablation. *Iraqi Journal of Applied Physics*, *19*(2), 3-8. https://www.iasj.net/iasj/article/260003.

[30] Jassim, A. S., Rashid, S. N. & Yaseen, H. M. (2020). Effect of CO_2 Laser Irradiation on the Topographic and Optical Properties of CdO Thin Films. *Baghdad Science Journal*, *17*(1), 318-328. https://dx.doi.org/10.21123/bsj.2020.17.1(Suppl.).0318.

[31] Wang, H., & Shadman, F. (2013). Effect of particle size on the adsorption and desorption properties of oxide nanoparticles. *AIChE Journal*, *59*(5), 1502-1510. https://doi.org/10.1002/aic.13936.

[32] Peng, S., McMahon, J. M., Schatz, G. C, Gray, S. & Sun, Y. (2010). Reversing the size-dependence of surface plasmon resonances. *Proceedings of the National Academy of Sciences*, *107*(33), 14530-14534. https://doi.org/10.1073/pnas.1007524107.

P- ISSN 1991-8941 E-ISSN 2706-6703 *Journal of University of Anbar for Pure Science (JUAPS)* Open Access
2024,(18), (02):203 – 212

توصيف جسيمات اوكسيد النيكل النانوية المحضرة بطريقة الاستئصال بالليزر النبضي: تقييم تأثير معلمات الليزر

بشرى محمد غضيب ، سحر ناجي رشيد *

قسم الفيزياء ، كلية العلوم ، جامعة تكريت ، تكريت ، العراق
email: sahar83@tu.edu.iq

الخلاصة:

إن تقنية الاستئصال بالليزر النبضي من أعلى إلى أسفل في السوائل هي عملية لها العديد من المزايا لتحضير الجسيمات النانوية. في هذا العمل تم تحضير جسيمات نانوية من صفيحة النيكل النقي عن طريق الاستئصال بالليزر النبضي في الماء منزوع الأيونات باستخدام ليزر Nd: YAG بثلاثة أطوال موجية (1064, 532, and 355 nm) و بثلاث طاقات (50, 100, and 150 mJ). بينت النتائج تكوين جسيمات النيكل النانوية بالإضافة إلى جسيمات أوكسيد النيكل النانوية ذات الأشكال الكروية وبمعدلات احجام تراوحت بين (14.3 – 18.44 nm). وقد وجد أن معدل الأكسدة يزداد عند استخدام الطول الموجي الأقصر لليزر في التحضير. ومن الواضح بشكل عام أن شدة الامتصاص ترتفع مع زيادة طاقة الليزر. من النتائج التي تم الحصول عليها فقد تبين ان افضل طول موجي مستخدم للتحضير هو (532 nm) اما الطاقة الافضل فهي (150 mJ). لقد أثبتت هذه التقنية الفيزيائية افضليتها من ناحية السهولة والكلفة القليلة لتحضير الجسيمات النانوية المعدنية واكاسيدها النانوية.

الكلمات المفتاحية :معلمات الليزر، NiONPs، PLAL، SPR